Electronic Supplementary Information for:

Acidic Nature of "NMR-invisible" Tri-coordinated Framework Aluminum Species in Zeolite

Shaohui Xin,[ad] Qiang Wang,*[a] Jun Xu,[a] Yueying Chu,[a] Pengfei Wang,[b] Ningdong Feng,[a] Guodong Qi,[a] Julien Trébosc,[c] Olivier Lafon,[ce] Weibin Fan[b] and Feng Deng*[a]

[a] *National Centre for Magnetic Resonance in Wuhan, State Key Laboratory of Magnetic Resonance and Atomic and Molecular Physics, CAS Key Laboratory of Magnetic Resonance in Biological Systems, Wuhan Institute of Physics and Mathematics, Chinese Academy of Sciences, Wuhan 430071, China*

[b] *State Key Laboratory of Coal Conversion, Institute of Coal Chemistry, Chinese Academy of Sciences, P.O. Box 165, Taiyuan, Shanxi 030001, P. R. China*

[c] *Univ. Lille, CNRS, ENSCL, UMR 8181, Unité de Catalyse et de Chimie du Solide 59000 Lille, France*

[d] *University of Chinese Academy of Sciences, Beijing 100049, China*

[e] *Institut Universitaire de France, 75231 Paris, France*

* E-mail: qiangwang@wipm.ac.cn; dengf@wipm.ac.cn

Table of Contents

Table S1. Relative percentages of different phosphoric species obtained by fitting the ^{31}P MAS NMR spectra.	**S3**
Table S2. Acquisition parameters for 2D and double-resonance NMR experiments.	**S4**
Table S3. ^{31}P and ^{27}Al chemical shifts obtained by DFT calculations.	**S5**
Figure S1. XRD patterns of parent NH_4-ZSM-5, calcined and hydrated H-ZSM-5, and subsequently dehydrated and TMPO adsorbed sample.	**S6**
Figure S2-S3. ^{29}Si MAS NMR analysis.	**S7- S9**
Figure S4. ^{1}H MAS spectra of parent and H-form ZSM-5 zeolites dehydrated at different temperatures.	**S10**
Figure S5. 2D ^{13}C {^{1}H} CP HETCOR, and ^{31}P {^{1}H} CP HETCOR MAS NMR spectra of dehydrated H-ZSM-5 zeolites with TMPO loading.	**S11**
Figure S6. 1D ^{27}Al MAS NMR spectra of hydrated H-ZSM-5, and dehydrated H-ZSM-5 with CH_2Cl_2-adsorbed.	**S12**
Figure S7. One-pulse ^{1}H spectra, and ^{1}H $\rightarrow$ ^{13}C CP MAS spectra of TMPO/H-ZSM-5 zeolites with the removal of solvent at different temperatures.	**S13**
Figure S8. One-pulse ^{27}Al spectra of TMPO/H-ZSM-5 zeolites with the removal of solvent at different temperatures.	**S14**
Figure S9. 2D ^{31}P {^{1}H} CP HETCOR MAS NMR spectrum of TMPO/H-ZSM-5 zeolites (Si/Al = 25) with the removal of solvent at 363 K.	**S15**
Figure S10. Sheared 2D ^{27}Al 3QMAS and selected normalized slices spectra of H-ZSM-5 zeolite with TMPO loading.	**S16**
Figure S11. 1D ^{31}P {^{27}Al} D-HMQC MAS NMR spectra of dehydrated and TMPO-loaded (P/Al=0.42) H-ZSM-5 zeolite with different recoupling time.	**S17**
Figure S12. 1D ^{31}P {^{27}Al} S-RESPDOR with two experiments being done at $B_0 = 11.7$ T.	**S18**
Figure S13. Simulations for S-RESPDOR with the consideration of multiple spins.	**S19-S20**
Figure S14. FT-IR spectra of pyridine adsorbed on H-ZSM-5 after evacuation at different temperatures.	**S21**
Figure S15. 1D one-pulse ^{31}P MAS spectrum, and 2D ^{31}P{^{1}H} HETCOR MAS NMR spectrum of dehydrated H-ZSM-5 zeolite (Si/Al = 140) with a low TMPO loading (P/Al = 0.23).	**S22**
DFT calculations	**S23**

Table S1. Relative percentages of different phosphoric species obtained by fitting the ^{31}P MAS NMR spectra of TMPO adsorbed on H-ZSM-5 (Si/Al=25) zeolites.

Samples	88ppm/%	85ppm/%	76ppm/%	69ppm/%	65ppm/%	51ppm/%
P/Al=0.42	—	9.33	61.34	5.80	21.22	2.30
P/Al=0.42 (h)[a]	—	—	70.99	4.77	16.77	7.47
P/Al=0.18	5.07	4.63	53.60	6.02	30.68	—
P/Al=0.18 (h)[a]	—	—	72.27	4.94	16.79	6.00

[a] The notation “(h)” represents exposure to humidity for 2 h.

Table S2. Acquisition parameters for 2D and double-resonance NMR experiments.

Pulse Sequence	**CP-HETCOR**		**PT-*D*-HMQC**	***D*-HMQC**	**DQ-SQ**	**FAM-3QMAS**	**S-RESPDOR**
Nuclei	$^{31}\mathrm{P}\ \{^{1}\mathrm{H}\}$	$^{29}\mathrm{Si}\ \{^{1}\mathrm{H}\}$	$^{31}\mathrm{P}\ \{^{27}\mathrm{Al}\}$	$^{27}\mathrm{Al}\ \{^{31}\mathrm{P}\}$	$^{27}\mathrm{Al}$	$^{27}\mathrm{Al}$	$^{31}\mathrm{P}\ \{^{27}\mathrm{Al}\}$
B_0 (T)	9.4	11.7	11.7	18.8	18.8	18.8	11.7
Number of scans	2048	2048	2400	5120	51200	4800	* [a]
t_1 increments (μs)	100.0	166.7	166.7	50.0	50.0	25.0	-
t_1 points	120	40	20	20	20	30	-
Recycle Delay (s)	1.0	1.0	1.0	0.5	0.3	0.2	2.0
ω_R (kHz)	10.0	6.0	6.0	20.0	20.0	40.0	6.0
o.d. rotor (mm)	4.0	7.0	7.0	3.2	3.2	1.9	7.0
^{1}H decoupling rf field (kHz)	50.0	50.0	62.0	100.0	-	-	62.0
Ramp CP							
Contact time (ms)	8.0	8.0	8.0	-	-	-	8.0
^{1}H channel rf field	62.5	41.7	49.0	-	-	-	49.0
X channel rf field	53.0	30.0	33.8	-	-	-	33.8
^{1}H $\pi/2$ pulse (us)	4.0	6.0	4.6	-	-	-	4.6
^{31}P $\pi/2$ & π pulse (us)	-	-	6.1 & 12.2	3.5 & 7.0	-	-	6.1 & 12.2
^{27}Al $\pi/2$ soft pulse (us)	-	-	10.0	8.0	8.0	10.4	-
Recoupling pulse	-	-	SR4	SR4	$\mathrm{BR}2_{2}^{1}$	-	SR4
Recoupling time (ms)	-	-	2.7	2.0	1.6	-	1.3 ~ 12.0

[a] The scan number for S-RESPDOR experiments was dependent on the sensitivity of corresponding ^{31}P MAS NMR spectra with different dephasing (mixing) times.

Table S3. ^{31}P and ^{27}Al chemical shifts obtained by DFT calculations.

Chemical shift/ppm	TMPO@BAS	TMPO@LAS	TMPO@B/L synergy
^{31}P	76	68	83
^{27}Al	54.4	49.6	56.4 (BAS) / 82.1 (LAS) *

* As shown in the local theoretically optimized structures (Fig. 6c), for TMPO adsorbed on the BAS with a neighboring unreacted tri-coordinated FAL site, the theoretically predicted ^{27}Al chemical shift was 56.4 ppm and 82.1 ppm for BAS and LAS respectively.

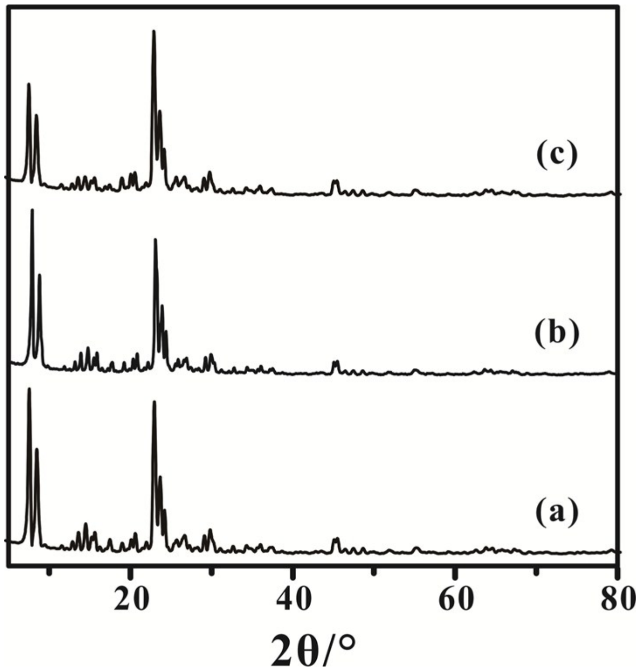

Figure S1. XRD patterns of (a) parent NH_4-ZSM-5, (b) calcined and hydrated H-ZSM-5, and (c) subsequently dehydrated and TMPO adsorbed sample.

^{29}Si MAS NMR analysis

The direct-excitation ^{29}Si MAS NMR spectrum of dehydrated zeolite in **Fig. S2a** can be deconvoluted into four characteristic resonances by Gaussian deconvolution. The major signals at approximately -113 ppm and -116 ppm were both associated with Q4 = [Si $(OSi)_4$] type silicon surrounded by four O-Si ligands. While the weak signals at -102 ppm and -108 ppm were due to Si with OH or Al in the second coordination sphere, and can be assigned to Q3 [1OH] = [Si $(OSi)_3(OH)$] and Q4 [1Al] = [Si $(OSi)_3(OAl)$] type silicons, respectively. This was confirmed by two (^{29}Si, ^{1}H) correlation peaks at (-102, 1.9) ppm and (-108, 4.0) ppm observed in its 2D ^{29}Si {^{1}H} HETCOR spectrum (**Fig. S2c**), where δ (^{1}H) = 1.9 ppm and 4.0 ppm were typical chemical shifts of protons (**Fig. S2b**) from Si-OH groups and Brønsted acidic sites, respectively. Quantitative analysis of 1D ^{29}Si MAS NMR spectra (F**ig. S3**) showed that only a slight loss (1%) of the integrated areas (*i.e.* relative concentration) of Q4[1Al] signal (14%) was observed on dehydrated H-ZSM-5 compared with that (15%) on parent NH_4-ZSM-5. Partially breaking of ≡Al-O- bond in the framework of zeolite during calcination and dehydration results in the formation of tri-coordinated framework aluminum.

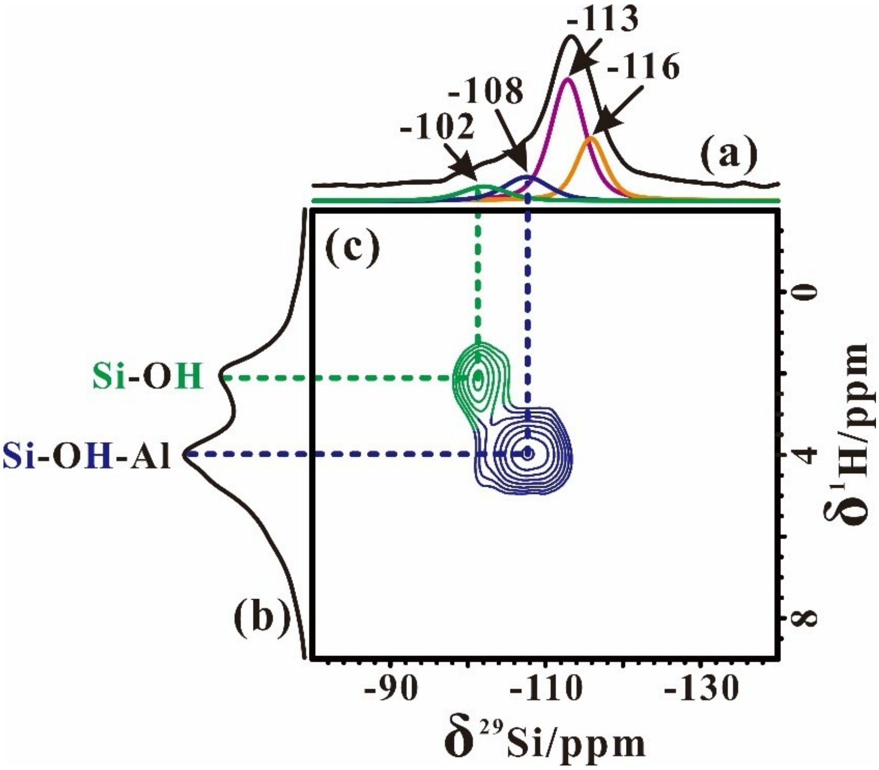

Figure S2. (a) One-pulse ^{29}Si MAS NMR spectrum with four deconvoluted peaks, (b) csecho ^{1}H MAS NMR spectrum, and (c) ^{29}Si {^{1}H} CP HETCOR MAS NMR spectrum of dehydrated H-ZSM-5 zeolite.

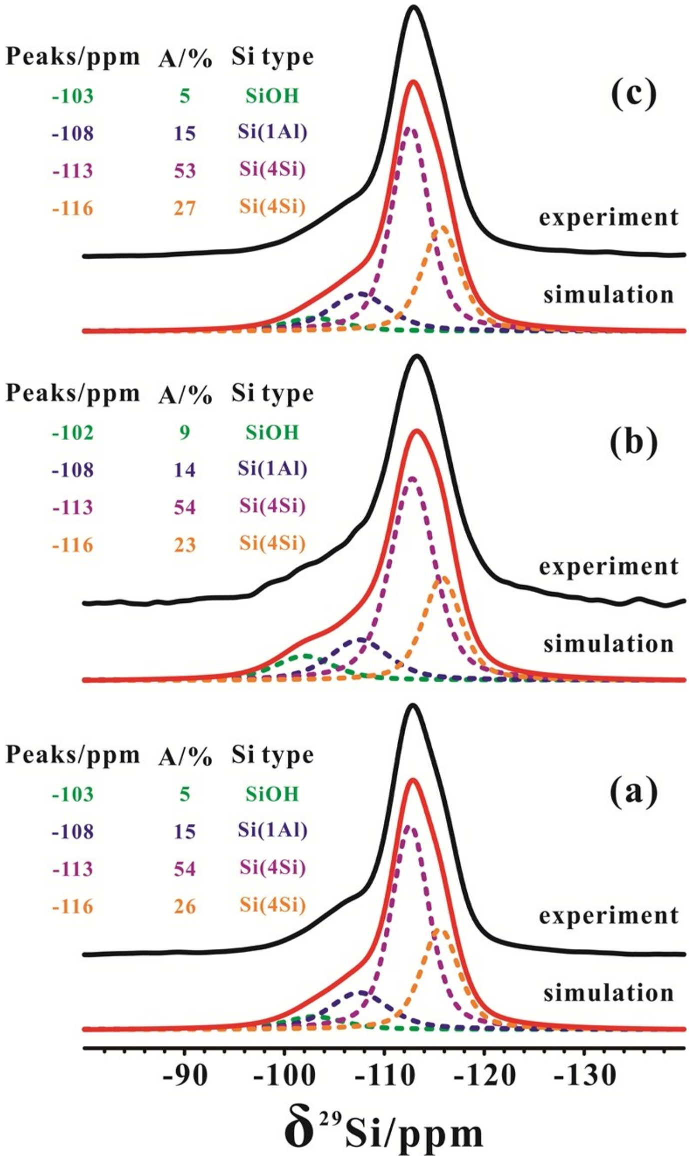

(c)

Peaks/ppm	A/%	Si type
-103	5	SiOH
-108	15	Si(1Al)
-113	53	Si(4Si)
-116	27	Si(4Si)

(b)

Peaks/ppm	A/%	Si type
-102	9	SiOH
-108	14	Si(1Al)
-113	54	Si(4Si)
-116	23	Si(4Si)

(a)

Peaks/ppm	A/%	Si type
-103	5	SiOH
-108	15	Si(1Al)
-113	54	Si(4Si)
-116	26	Si(4Si)

Figure S3. ^{29}Si MAS NMR spectra of (a) parent NH_4-ZSM-5, (b) calcined and dehydrated H-ZSM-5, and (c) rehydrated H-ZSM-5 with decomposed peaks of specific Si and corresponding contents.

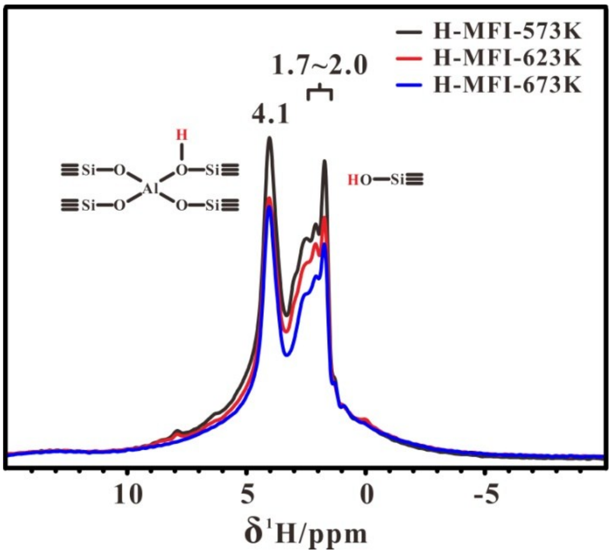

Figure S4. 1D one-pulse ^{1}H spectra of H-form ZSM-5 zeolites dehydrated at 673 K (blue line), 623 K (red line), and 573 K (black line).

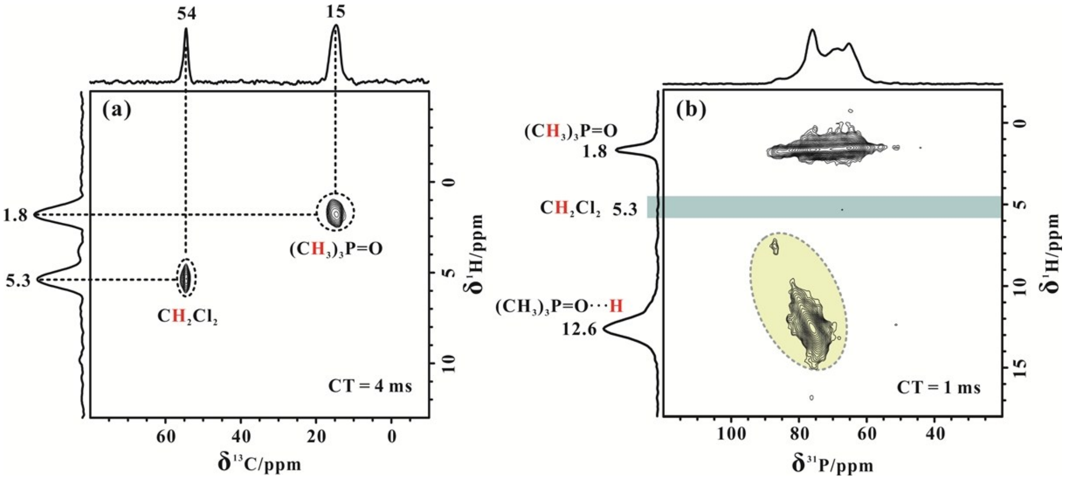

Figure S5. (a) 2D ^{13}C {^{1}H} CP HETCOR, and (b) ^{31}P {^{1}H} CP HETCOR MAS NMR spectra of dehydrated H-ZSM-5 zeolites (Si/Al = 25) with a TMPO loading of P/Al = 0.18, CH_2Cl_2 removal at 323 K.

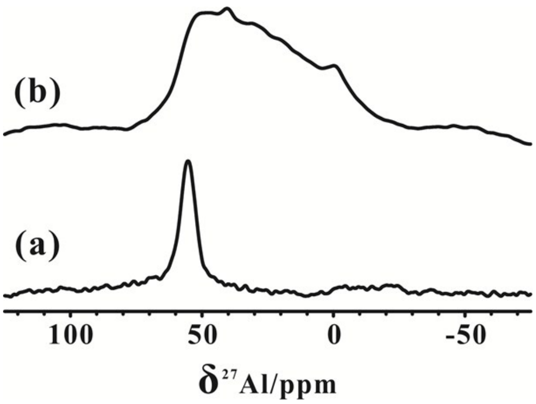

Figure S6. 1D ^{27}Al MAS NMR spectra of hydrated H-ZSM-5 (a), and dehydrated H-ZSM-5 with solely adsorbed CH_2Cl_2 (b), all experiments were recorded at B_0 = 11.7 T.

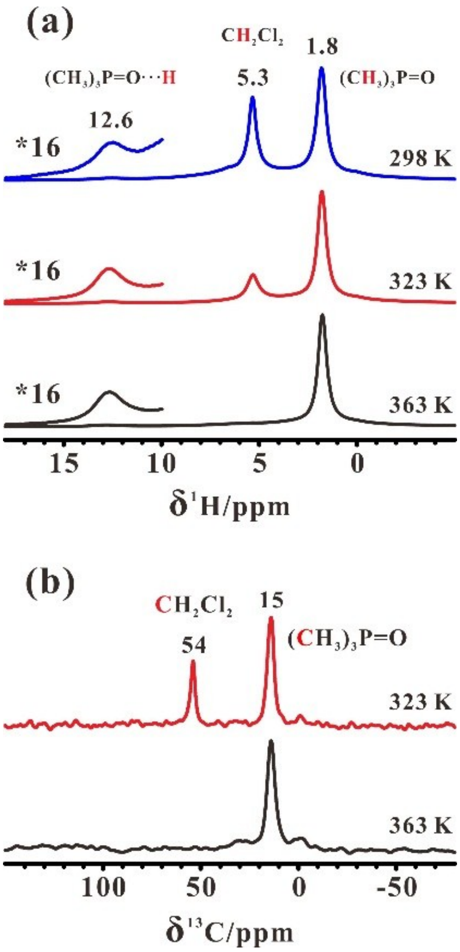

Figure S7. (a) One-pulse ^{1}H spectra, and (b) ^{1}H → ^{13}C CP MAS spectra of dehydrated H-ZSM-5 zeolites (Si/Al = 25) with a TMPO loading of P/Al = 0.18 (CP contact time of was 2 ms). Solvent CH$_2$Cl$_2$ was removed at 298 K (blue line), 323 K (red line), 363 K (black line).

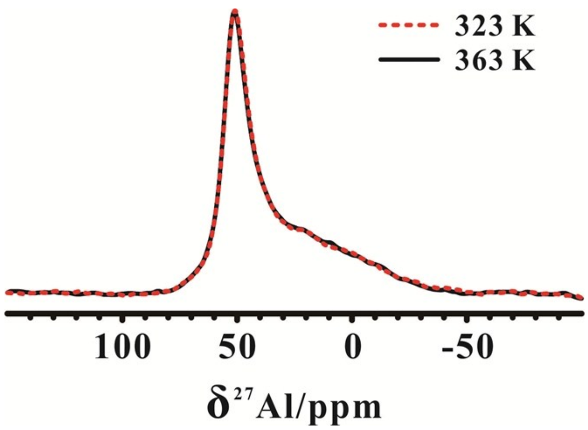

Figure S8. One-pulse ^{27}Al spectra of dehydrated H-ZSM-5 zeolites (Si/Al = 25) with a TMPO loading of P/Al = 0.18. Solvent was removed at 323 K (red dashed line), 363 K (black line).

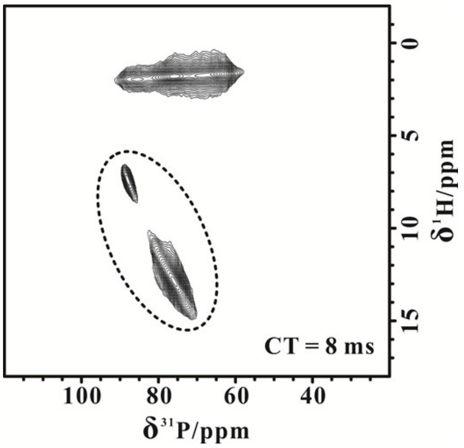

Figure S9. 2D ^{31}P {^{1}H} CP HETCOR MAS NMR spectrum of dehydrated H-ZSM-5 zeolites (Si/Al = 25) with a TMPO loading of P/Al = 0.18. Solvent CH_2Cl_2 was removed at 363 K.

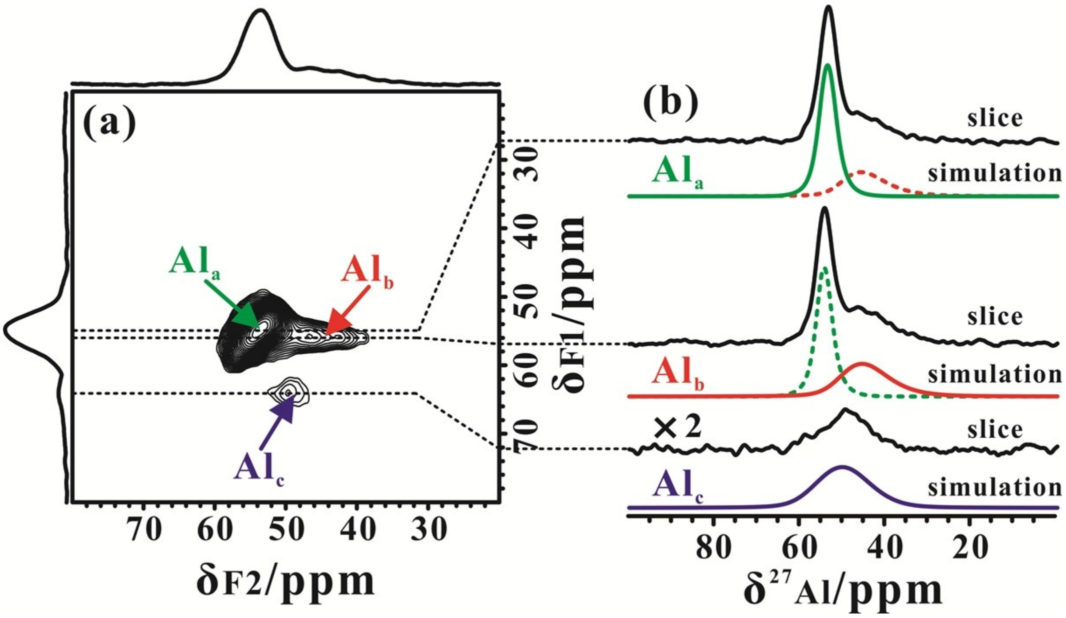

Figure S10. (a) Sheared 2D ^{27}Al 3QMAS and (b) selected normalized slices spectra of H-ZSM-5 zeolite with a low TMPO loading (P/Al=0.18). Skyline projections are shown along F1 and F2.

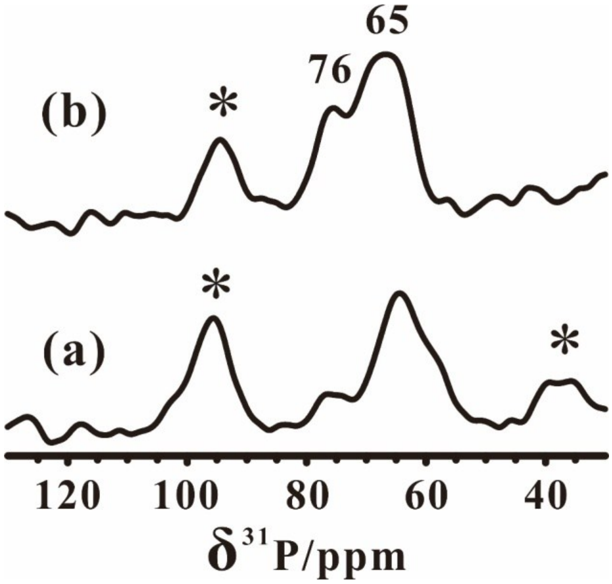

Figure S11. 1D ^{31}P {^{27}Al} D-HMQC MAS NMR spectra of dehydrated and TMPO-loaded (P/Al=0.42) H-ZSM-5 zeolite recorded at 11.7 T with different recoupling time: (a) τ_{mix} = 1.33 ms, (b) τ_{mix} = 2.67 ms. The asterisks denote spinning sidebands.

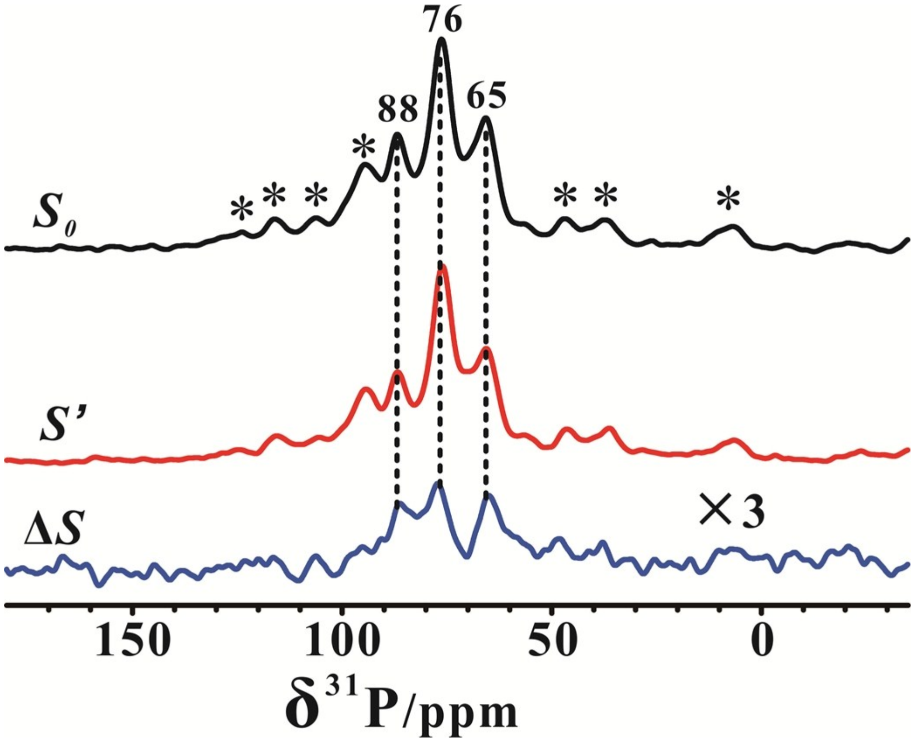

Figure S12. 1D ^{31}P {^{27}Al} S-RESPDOR with two experiments being done at B_0 = 11.7 T: S' and S_0, with or without the ^{27}Al irradiation pulses, respectively. The S-RESPDOR fraction is equal to $\Delta S/S_0 = (S_0 - S')/S_0$. The carrier frequency on ^{31}P channel was set at 88 ppm and the number of scan was set to 2000. The asterisks denote spinning sidebands.

Simulations for S-RESPDOR with the consideration of multiple spin systems

Analogous to our previous studies,[1] the ideal case was firstly considered assuming that the heteronuclear dipolar dephasing is only from an isolated nuclear spin pair. This allows us to know the average interactions/distances between the different phosphorus and aluminum atoms. However, the analytical formula was deduced based on an ideal spin pair without any consideration of experimental conditions, we also performed numerical simulations with SIMPSON software, which can simulate the dephasing curve by taking the experimental parameters of the S-RESPDOR pulse sequence such as pulse lengths, RF fields, delays between pulses *etc*. into account. The powder averaging was accomplished using 6080 orientations: 320{α, β}-pairs & 19 γ-angles. The 320{α, β}-pairs that relate the molecule and rotor frames were selected according to the REPULSION algorithm. In addition to the isolated spin pair with the ^{31}P-^{27}Al distance of 2.9 Å (Fig. S13a) used in above analysis, the effects of dipolar network of multiple spin systems on the ^{31}P-^{27}Al dipolar dephasing of the Lewis complex [$(CH_3)_3PO{\bullet}{\bullet}Al{\equiv}$] were explored by additional numerical simulations as well. There is an additional ^{31}P spin with a longer distance (here set to 4.2 Å, Fig. S13b) away from ^{31}P spin than that of the initial ^{31}P-^{27}Al spin pair, and the distance between two ^{31}P spins is set to 4.8 Å which could be thought as a relative short distance between two TMPO molecules in H-ZSM-5 zeolite. We also assumed there is an additional ^{27}Al spin with a longer distance (here set to 3.8 Å,) away from ^{31}P spin than that of the initial ^{31}P-^{27}Al spin pair, and the distance between two ^{27}Al spins is set to 3.6 Å which could be thought as the closest distance in zeolite framework with the "-Al-O-Si-O-Al-" sturcture, and different quadrupolar coupling constants (2 MHz in Fig. S13c and 16 MHz in Fig. S13d) were set for the additional ^{27}Al spin.

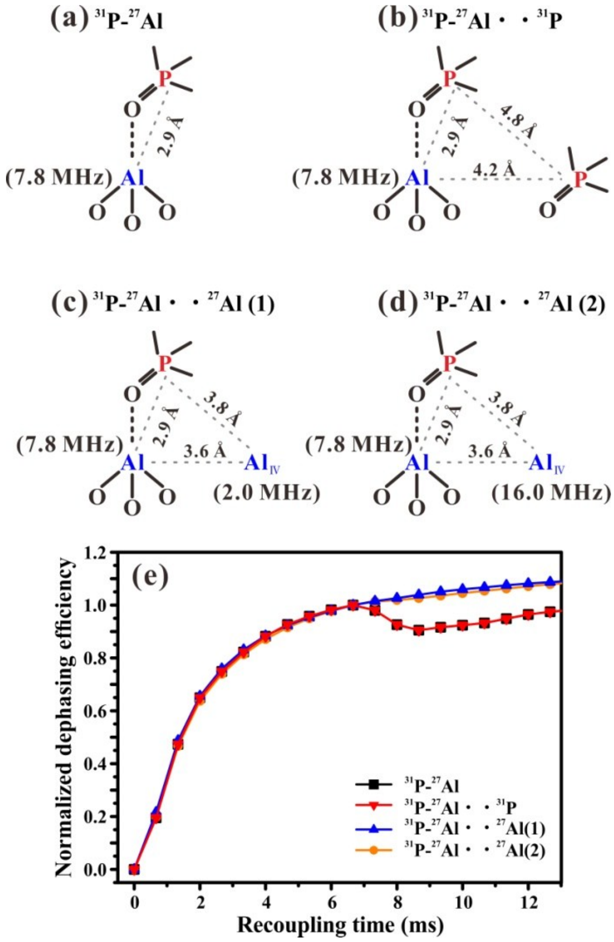

Figure S13. The structure models of (a) isolated ^{31}P-^{27}Al spin pair, (b) ^{31}P-^{27}Al with a neighboring ^{31}P nucleus, (c) ^{31}P-^{27}Al with a neighboring ^{27}Al nucleus (C_Q = 2 MHz), (d) ^{31}P-^{27}Al with a neighboring ^{27}Al nucleus (C_Q = 16 MHz), and (e) Normalized S-RESPDOR signal fractions for spin pair (a) (-■-), spin pair (b) (-▼-), spin pairs (c) (-▲-) and spin pairs (d) (-●-). The parameters used in SIMPSON simulations are the same as that in our experiments.

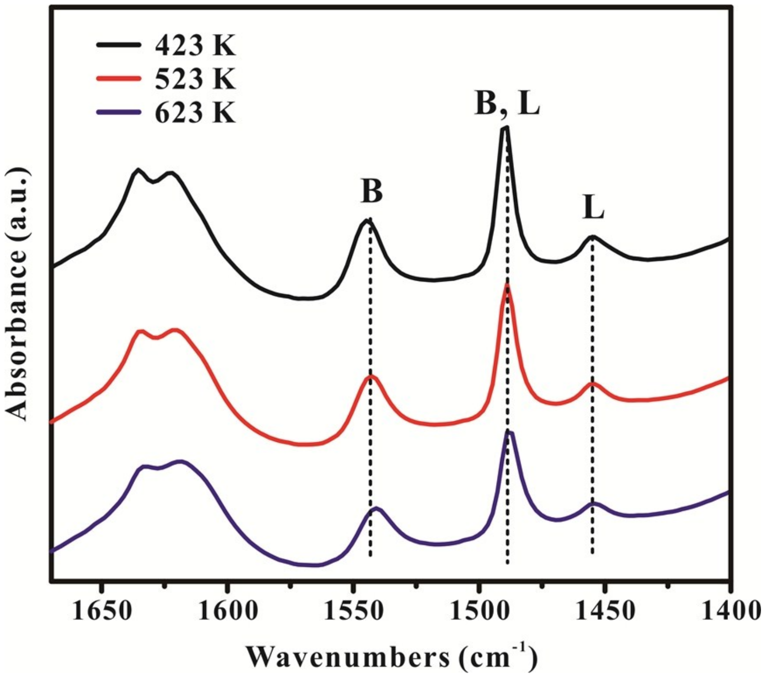

Figure S14. FT-IR spectra of pyridine adsorbed on H-ZSM-5 after evacuation at different temperatures. The B and L peaks represent pyridine adsorbed on Brønsted and Lewis acid sites, respectively.

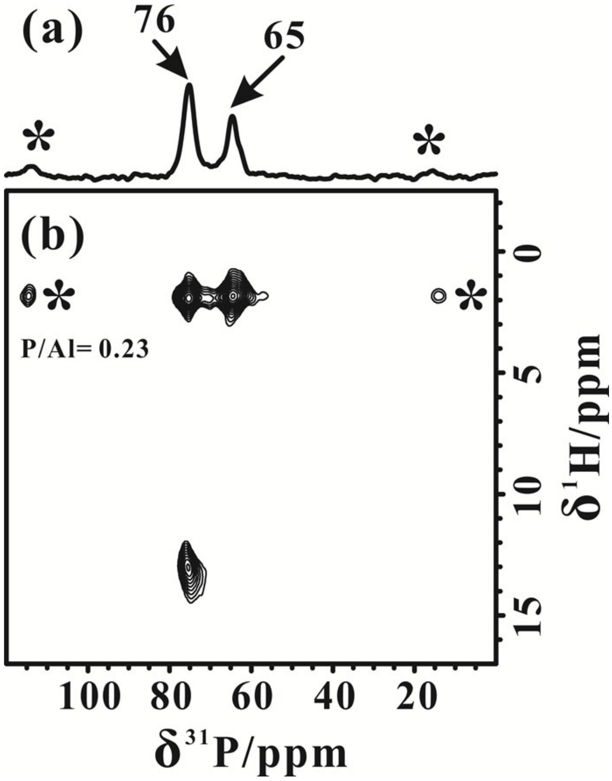

Figure S15. 1D one-pulse ^{31}P MAS spectrum (a), and 2D ^{31}P{^{1}H} HETCOR MAS NMR spectrum (b) of dehydrated H-ZSM-5 zeolite (Si/Al = 140) with a low TMPO loading (P/Al = 0.23).

DFT calculations

For the isolated Brønsted site (**Fig. S16a**) in a 64 T cluster model, the substituted Al atom is usually placed at the T12 site,[2] which resides at the interaction of the straight and sinusoidal channels of ZSM-5. For the Brønsted/Lewis synergetic site, an additional Al is placed at the T7 site to represent the tri-coordinated FAL (**Fig. S16b**). Then, we optimized the structures of TMPO molecules adsorbed on BAS and calculated the ^{31}P chemical shifts.

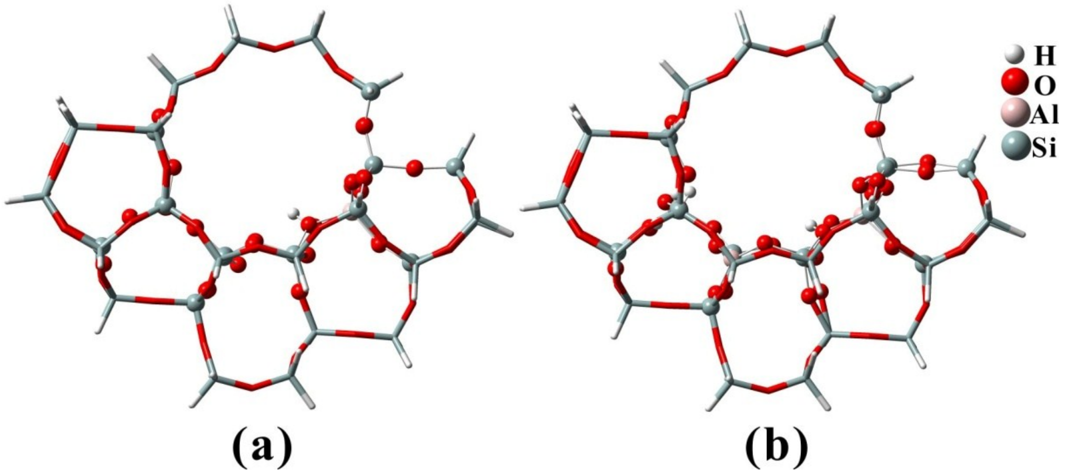

Figure S16. View along the [010] axis of 64 T MFI structure to model isolated Brønsted acid site with Al located at the T12 site (a) and Brønsted/Lewis synergetic acid site with tri-coordinated framework Al located at the T7 site (b). The 24 T active site atoms are treated as the high-layer.

References

1. G. Qi, Q. Wang, J. Xu, J. Trebosc, O. Lafon, C. Wang, J. P. Amoureux and F. Deng, *Angew. Chem. Int. Ed.*, 2016, **55**, 15826-15830.
2. S. Svelle, C. Tuma, X. Rozanska, T. Kerber and J. Sauer, *J. Am. Chem. Soc.*, 2009, **131**, 816-825.